Wide-band Radio Frequency Measurements: From Instrumentation to Sampling Theory

Charles Nader, *Member, IEEE,* Wendy Van Moer, *Senior Member, IEEE,* Niclas Björsell, *Member, IEEE,* Peter Händel, *Senior Member, IEEE,*

***Abstract*—For the past several decades, measuring a broad-band wireless signal accurately has been of major concern to the industry as well as the academic world. From Nyquist and Shannon till today's major suppliers of state-of-the-art measurement equipments, finding methods to improve the measurement bandwidth and resolution has always been the ultimate goal of a scientific race. This race is kept alive by the "never ending" need for wider bandwidths and larger dynamic ranges in a world moving from kHz to GHz scale. In the past, several sampling techniques and measurement setups have been developed to measure the time domain waveform of different signal classes ranging from periodic to real-time signals. However, most of the developed measurement techniques were characterized by high cost and limited to a special application. Nowadays, more research is focused on designing a low cost, wide-band measurement setup with large dynamic range, and suitable for multiple applications/tasks.**

This article presents a survey of the major wide-band, time domain measurement systems of today's market. A detailed explanation of their architecture, their sampling technique, possible applications, as well as their advantages/disadvantages, challenges/limitations, is given. In addition, a glance into the latest scientific findings in the field and how measurement systems are evolving, is presented.

I. Overview of wide-band Radio frequency receivers

No matter if the purpose targets listening to radio or testing developed wireless devices, for civilian or military applications, based on terrestrial or spacial links, a radio frequency (RF) receiver, with good measurement capabilities that preserves the received signal information, is required. Today's RF measurement receivers with wide-band capabilities are split into two groups based on the measurement strategy they adopt. Both groups result in a time domain waveform, with both amplitude and phase information, that is constructed either from a transformation of its frequency contents or directly from its time domain samples.

C. Nader used to be with the Department of Electronics, Mathematics and Natural Sciences, University of Gävle, Gävle, SE-80176, Sweden, and also with the Signal Processing Lab, ACCESS Linnaeus Center, Royal Institute of Technology, Stockholm, SE-10044, Sweden and with the ELEC Department, Vrije Universiteit Brussel, B-1050 Brussels, Belgium. Presently, he is with the Department of Systems Engineering, Focubeam GmbH, D-89081 Ulm, Germany.

W. Van Moer and N. Björsell are with the ELEC Department, Vrije Universiteit Brussel, B-1050 Brussels, Belgium and with the Department of Electronics, Mathematics and Natural Sciences, University of Gävle, Gävle, SE-80176, Sweden.

P. Händel is with the Signal Processing Lab, ACCESS Linnaeus Center, Royal Institute of Technology, Stockholm, SE-10044, Sweden, and also with the Department of Electronics, Mathematics and Natural Sciences, University of Gävle, Gävle, SE-80176, Sweden.

Corresponding author: charles.nader@focubeam.com.

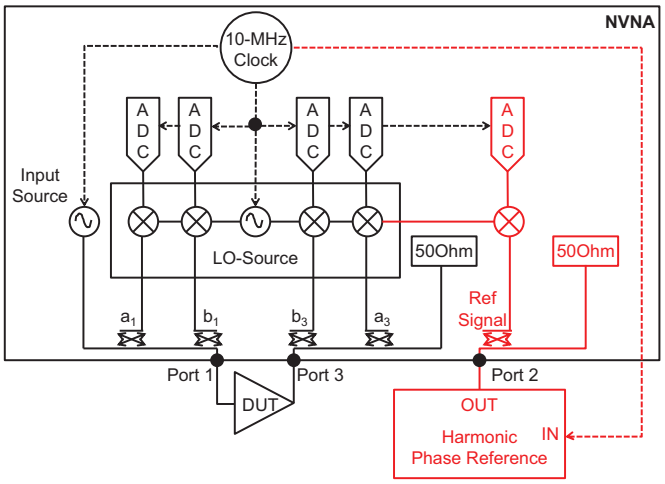

Fig. 1: Simplified block diagram of an NVNA showing the heterodyne architecture for measuring the incident and reflected waveforms of a two-port device-under-test (DUT).

A. Sweeping receivers

The first group of receivers, which is based on an heterodyne architecture, sweeps over the frequency band of interest and measures one frequency component of the incident waveform at a time. The mixer-based nonlinear vector network analyzer (NVNA) [1]–[3] is an example of this group, which we denote as *sweeping-based* receivers. Since collecting the information about the waveform is done in steps, receivers belonging to this group are only dedicated for measuring periodic signals. The main architecture of sweeping-based receivers is to down-convert a narrow-band filtered portion of the incident waveform to baseband and measure its content with a narrow-band high resolution analog-to-digital converter (ADC). The down-conversion to baseband is done by using an RF mixer and a local oscillator (LO) source. Hence, such receivers are sometimes referred to by engineers as mixer-based receivers. A simplified block diagram of a mixer-based NVNA is shown in Fig. 1.

Due to the narrow-band characteristic of the measurements in a sweeping-based receiver, the noise level is greatly low. Hence, a large dynamic range is achieved. However, a major challenge that is faced by such a type of receivers, is the loss of phase coherency due to the sweeping operation. In order

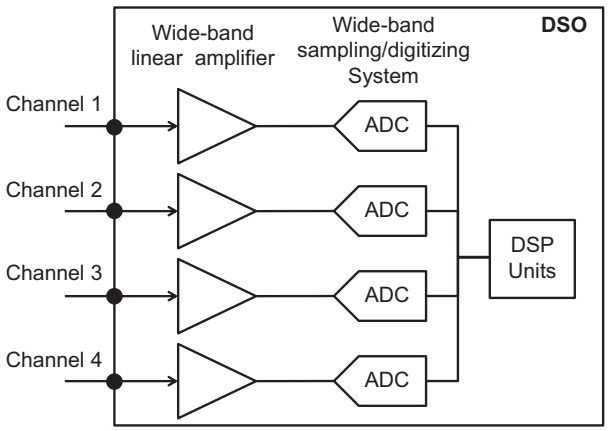

Fig. 2: Simplified block diagram of a DSO showing the direct RF-sampling.

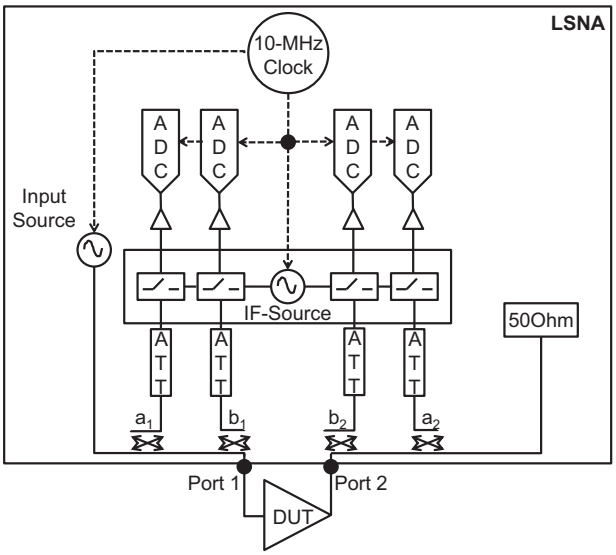

Fig. 3: Simplified block diagram of an LSNA showing the sampler-based down-conversion architecture.

to preserve phase information through the measurements and reconstruct the time domain wide-band waveform, a harmonic phase reference and a reference mixer are used to lock the relative phase information during the sweeping procedure. From Fig. 1 it can be seen that the phase synchronization during the sweeps is achieved through an additional mixer and a harmonic phase reference located at port two. Such phase synchronization strategy requires accurate calibration and special hardware design which can be expensive [4].

B. Sampling receivers

The second group of wide-band measuring receivers is based on capturing instantaneously all the frequency components of the waveform by taking samples over time. The sampling can be done at RF level or intermediate frequency (IF) level depending on the available analog bandwidth of the sampler that is used [5]–[10]. Hence, we denote the measurement strategy as *sampling-based* measurement. The main advantage of the sampling-based measurement technique compared to the sweeping-based is the fact that since the whole spectrum of the incident waveform is measured in one single take, there is no need for relative phase synchronization between the spectral components, as is the case for sweeping-based measurement systems. Hence, the receivers hardware architectures are more simple and their respective measurements are much faster [4]. However, on the cost of a lower resolution due to the wide-band characteristic of the measurement which increases the noise level.

Measurement receivers fitting the second group are split into two categories depending on the analog bandwidth of their front-end, RF-sampling or IF-sampling. Some of them can measure real-time signals, while others are limited to repetitive or periodic signals, depending on their sampling rate capabilities. In the following, an overview of the major measurement receiver architectures using a sampling-based measurement technique is given.

1) RF-sampling receivers: A receiver belongs to the RF-sampling category when the sampling operation is applied directly to the incident RF waveform. Hence, RF-sampling receivers require a wide-band analog front-end [5]–[7], [9]. The sampling rate can be higher than the Nyquist rate of the waveform to measure, as in the case of real-time sampling scenarios [7], [9], or at a sampling rate lower than the Nyquist rate of the waveform to measure, undersampling, as in the case of periodic or repetitive scenarios [5]–[7]. In addition, the sampling operation can be applied by an expensive wide-band high sampling rate ADC which is denoted by direct RF-sampling, e.g. real-time digital sampling oscilloscope (DSO), or through the combination of a wide-band slow sampler and a relatively narrow-band high resolution ADC which is denoted by sampler-based down-conversion, e.g. large signal network analyzer (LSNA). Figures 2 and 3 show the simplified block diagrams of two RF-sampling based receivers designed respectively for measuring real-time and periodic signals. In Fig. 2, the waveform is first amplified by an expensive wide-band linear amplifier, sampled/digitized by an expensive wide-band high sampling rate ADC, and then processed in digital signal processing (DSP) units [7], [9]. In Fig. 3, the waveforms are first conditioned through attenuators (ATT), down-converted/compressed by wide-band samplers, then amplified by narrow-band linear amplifiers and digitized by high resolution ADCs [4].

It should be noted that the measurement bandwidth of a real-time measurement receiver is set by its sampling rate. The measurement bandwidths reported in today's market are beyond 33 GHz [9], i.e., 63 GHz based on [2] using highly expensive indium phosphide (InP) based circuits [9], which has superior electron velocity offering very high operating range up to hundreds of GHz. For a wide-band receiver dedicated for measuring periodic waveforms, it is the analog bandwidth of its sampler that sets its measurement bandwidth. A typical bandwidth reported in today's market for such application is around 50 GHz. In Section II, more insights into the analog front-end architecture and challenges of wide-band receivers/ADCs are given.

Comparing both RF-sampling receiver architectures, the

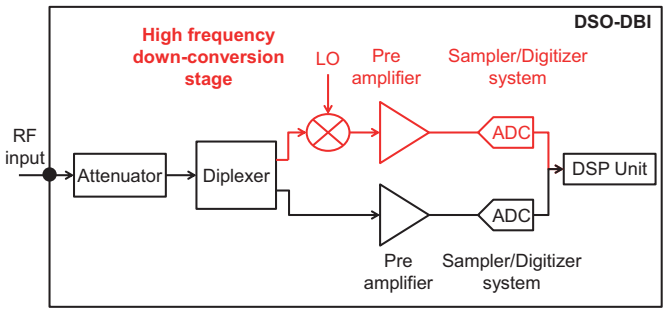

Fig. 4: Simplified block diagram of a single channel real-time DSO based on digital bandwidth interleave (DBI) showing the IF-sampling.

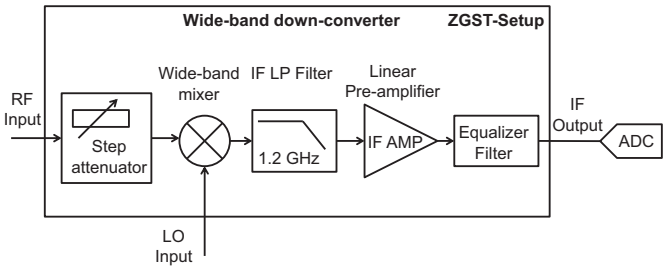

Fig. 5: Simplified block diagram of an IF-sampling measurement receiver using the Zhu-Frank generalized sampling theorem (ZGST).

main advantage of applying the direct RF-sampling is to measure real-time signals. Another advantage is the amplification of the signal before sampling which leads to higher dynamic range and less noisy data. In case of sampler-based down-conversion receivers, the output waveform of the sampler consists of the compressed RF signal and the compressed/aliased wide-band noise. Hence, amplifying the signal will also amplify the noise, which leads to low signal-to-noise ratio (SNR). The main reason for moving the amplification stage from the front-end to behind the sampler is the unavailability of wide-band linear amplifiers covering the measurement bandwidth at reasonable price.

2) IF-sampling receivers: A receiver belongs to the IF-sampling category when the sampling operation is applied at an intermediate stage after down-conversion through a mixer. Such type of receivers are designed either to overcome limitations on the RF analog front-end, in particular the availability of a wide-band linear pre-amplifier as in [8], or to measure the wide-band information carried by an RF carrier as in [10]. Such type of receivers requires the design of a linear mixer with wide-band capabilities relative to the application. The sampling operation itself can be at a rate higher than the Nyquist rate of the IF waveform, as for the cases of real-time sampling scenarios [8], or at a rate lower than the Nyquist rate of the waveform to measure, as for the cases of repetitive or periodic waveform scenarios [10]. Figures 4 and 5 show the simplified block diagrams of two IF-sampling based receivers designed respectively for measuring real-time and repetitive waveforms.

It should be noted that the first setup shown in Fig. 4 uses the technique of digital bandwidth interleave (DBI) to overcome the front-end analog bandwidth limitation [8]. Hence, the RF incident waveform is spectrally split using a diplexer into parallel channels which are down-converted to fit the analog bandwidth of the pre-amplifiers. The resulting IF waveforms are then amplified and digitized using time interleaved ADCs. Data collected from the ADCs are then processed/combined in the digital signal processing (DSP) units to reconstruct digitally the incident waveform [8]. The analog bandwidths reported in today's market based on DBI are beyond 45 GHz, i.e., 65 GHz based on [11]. A drawback of such measurement setup is the need for a pre-amplifier and a set of time-interleaved ADCs for every parallel channel which increases the size, the power dissipation and the price.

In addition, accurate phase synchronization needs to be done when reconstructing the wide-band RF waveform. The main strategic difference between the measurement setup presented in Fig. 4 and the one describe in Fig. 2, is that the first strategy focuses on the improvement in DSP technologies, while the latter focuses on new and expensive material for state-of-the-art integrated circuits (ICs) design.

The second measurement setup presented in Fig. 5 is dedicated for measuring bandlimited waveforms. The RF signal is first conditioned through a stepping attenuator to fit the linear operating range of the down-conversion mixer. After mixing, the signal is filtered to eliminate all down-conversion spurious and then amplified through linear amplifiers. Equalization and filtering are then applied to correct for the measurement system effects. The output IF signal is then undersampled using a high resolution ADC based on the Zhu-Frank generalized sampling theorem (ZGST) [10].

II. Analog-to-Digital Converters

The most important key element for sampling-based measurements is the ADC system. The ADC system refers to the pre-amplifier, sampler and quantizer as a whole package. Its analog bandwidth, sampling rate and resolution, capabilities or limitations, have shaped many of the measurement techniques described in the previous section. Hence, in this section the main characteristics of an ADC system are presented. Challenges facing its application to wide-band measurements are discussed. In particular, the trade-off between its sampling rate and resolution, its analog bandwidth limitation, and its high cost will be investigated.

A. Working principle

In general, an ADC system consists of four main blocks which define its performance. A simplified schematic is presented in Fig. 6. The continuous analog signal passing through the low pass filter, which sets the analog bandwidth of the ADC, is first amplified and then buffered to charge the capacitor of the sample and hold circuit when the switch is closed. When the switch is open, the discrete analog signal is buffered to the quantizer which transforms it to discrete digital levels. The trigger signal of both the switch and the quantizer is controlled by the sampling clock which can be generated externally or internally [12]. In the following, the main characteristics and working principle of each block of the ADC system are presented.

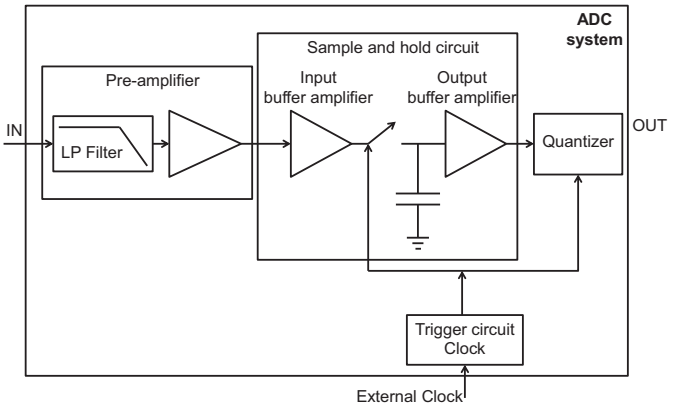

Fig. 6: Simplified block diagram of an ADC system.

1) Pre-amplifier: The first block is the pre-amplifier which conditions the amplitude of the incident waveform to fit the full scale of the quantizer. Hence, the best resolution is achieved with the highest SNR. The main characteristics of the pre-amplifier are good linearity and gain flatness over the operating analog bandwidth of the ADC, as well as a fast slew rate in order to amplify fast variations in the signal.

2) Sample and hold circuit: The second block in an ADC system is the sample and hold circuit which transforms the time continuous analog waveform to time discrete analog samples ready to be quantized. The main characteristics of the sample and hold circuit are its analog bandwidth, i.e. its bandwidth of operation, and its sampling rate. A sample and hold circuit usually consists of an input amplifier buffer, a switch, a capacitor, and an output amplifier buffer. The switch is usually controlled by a trigger which sets its switching rate. When the switch is closed, the input amplifier buffers the input signal by showing a high impedance at its input and providing sufficient current gain to charge the capacitor. When the switch is open, the charge in the capacitor is held constant for a certain time required to complete the conversion in the quantizer, i.e. conversion time. Hence, the role of the output amplifier buffer is showing a high impedance to the hold capacitor in order to prevent it from discharging [13], [14].

3) Quantizer: The third block in an ADC system is the quantizer which maps the time discrete analog levels to time discrete digital levels. The digital levels are determined by the number of bits available in the quantizer, e.g. a quantizer with 12-bits offers 2^{12} digital/quantization levels. Usually, the mapping between the analog levels and the quantization levels is done based on a rounding operation or a truncation operation. The resolution of a quantizer, called amplitude resolution, is the ratio between the peak-to-peak analog amplitude the quantizer can handle, called full scale, and the number of quantization levels. Hence, in order to measure very small amplitude variations in the analog signal, a high amplitude resolution is needed which requires a large number of quantization bits. The operation of mapping an analog value that have an infinite resolution to a discrete digital level with a fixed resolution, i.e. the quantization resolution, causes rounding, which is usually denoted by quantization error [15]. The quantization error can be seen as a noise level added to the input analog value. Reducing the quantization error requires a fine resolution, hence a large amount of bits. However, for a direct conversion technique, such as Flash converters, the resolution is constrained by the die size, power consumption and high demands on precise matching between comparators whose numbers are proportional to the quantization levels. Hence, high amplitude resolution requires other converter architectures, e.g. cascaded digital comparators, which leads to more complicated circuits and longer quantization time, that limits the sampling rate [13], [14].

4) Trigger circuit: The forth block in an ADC system is the trigger circuit which controls the switching of the sample and hold circuit and the quantization circuit. The triggering rate is controlled by the sampling clock of the ADC which can be generated internally through a clock IC based on a FracN synthesizer or externally through a sampling clock source. An important characteristic of the trigger circuit, and hence of the sampling clock, is its stability. Any time drift, or clock inaccuracy, causes deviation from the precise sample timing intervals, which is denoted by jitter. As a result, the positions of the analog signal samples become irregular, which causes reconstruction or analysis errors in the data processing that degrade the SNR. Such phenomenon, sensitivity to time based distortion, is more critical when measuring real-time wide-band signals with fast sampling rates [13], [14].

B. ADC limitations and challenges

ADCs used in today's RF systems face four challenges that need to be overcome in order to catch up with the market demands on higher data rate and wide-band measurement capabilities [16]: 1. the availability of a high amplitude resolution; 2. the availability of a high sampling rate; 3. the availability of wide analog bandwidth; 4. achieving the previous requirements in a cheap way.

1) Amplitude resolution: Due to the high demands on data, today's wireless systems use sophisticated modulation schemes which are characterized by large peak-to-average-power ratios (PAPRs). Such large PAPRs put high demands on the full scale range of the ADC. Hence, in order to keep a good amplitude resolution, large numbers of quantization bits are required. Unfortunately, as presented previously, this means slow sampling rate ADCs.
2) Sampling rate: Due to the high demand on data, today's wireless systems are using wide-band modulated signals. In addition, RF systems are moving toward software defined radios where several wireless systems use the same analog front-end. Hence, ADCs with wide-band sampling capabilities are needed, e.g., testing and characterizing nonlinear RF components whose output signal spectrum spreads significantly. Unfortunately, achieving high sampling rates with today's ADCs leads to a reduction in the amplitude resolution. Hence, a trade-off exists between the sampling rate and the amplitude resolution.
3) Analog bandwidth: When measuring wide-band waveforms, two major blocks in an ADC circuit face critical

challenges. The pre-amplifier and the sampler need to maintain a linear behavior and a flat response over the whole measurement bandwidth. Unfortunately, such demands are difficult to satisfy with today's technology. Hence, new IC technologies are required.

4) Cost: Achieving all the above demands, from high resolution, to fast sampling rate and wide analog bandwidth, leads to complex designs based on expensive materials, which increase the overall cost of the ADC, and hence of the RF system using it. Therefore, it is desirable to use DSP to overcome some of the hardware challenges and reduce in the overall cost.

III. Sampling techniques

Based on the application of interest, e.g. measuring real-time or periodic signals, a sampling technique need to be chosen. Based on that sampling technique, a measurement system is used. This section presents a short overview of the main sampling techniques that had impact on RF measurement receivers, from basics to the latest state-of-the-art, with their applications and limitations.

A. Nyquist-Shannon sampling

The origin of sampling goes back to 1928 when Henry Nyquist described the sampling criteria for correctly reconstructing a signal from its measured samples. Briefly, the Nyquist sampling theorem states that in order to correctly reconstruct a signal, the sampling frequency, f_s, needs to be at least two times bigger than the highest frequency component in the waveform f_{max}, [17]. Hence, based on Nyquist, the largest measurable frequency is equal to half the sampling rate $f_s/2$, which is referred to as the Nyquist frequency and sets the digital bandwidth of an ADC. In addition, the consecutive frequency zones, starting from DC, and of bandwidth $f_s/2$, are called Nyquist zones, e.g. the frequency band from DC to $f_s/2$ is called first Nyquist zone, the frequency band between $f_s/2$ and f_s is referred to as second Nyquist zone, and so on. Based on Nyquist, any frequency component of the waveform that is above the first Nyquist zone will appear in its reconstructed image as a low frequency component in the first Nyquist zone. Such phenomenon is referred as aliasing. Nyquist sampling is mainly used in today's wide-band oscilloscopes when measuring real-time signals. Hence, it is sometimes referred to as real-time sampling. Usually a sampling rate much higher than the bound set by Nyquist is chosen in order to accurately represent the waveform, especially if the waveform contains fast varying dynamics with high PAPR. The operation of increasing the sampling rate beyond Nyquist is called oversampling.

The lower bound set by Nyquist on the sampling rate was later on relaxed for modulated signals by Claude Shannon, who limited the lower bound to the bandwidth of the waveform rather then its highest frequency component [18]. If the waveform contains frequencies spreading between a minimum frequency f_{min} and f_{max}, then the sampling rate should be two times bigger or equal to their difference. In addition, the sampling frequency should be chosen such that the spectrum of the waveform fits completely in a Nyquist zone. For the case when f_{min}=0 Hz, the Shannon sampling theorem resumes to Nyquist criterion. Hence, the conditions set by both scientists are referred nowadays by Nyquist-Shannon sampling theorem or by bandpass sampling.

In some of the Â§Â§Â§literatures, the Nyquist-Shannon criterion is presented based on a strict bound. Hence, the equality is omitted, as measuring a frequency at DC or $f_s/2$ can lead to ambiguities in amplitude and phase. Such ambiguities will affect all multiples of the Nyquist frequency when measurement setups based on undersampling are used [19], [20]. As a result, those frequencies, multiples of the Nyquist frequency, are denoted as critical frequencies. More details about the critical frequencies will be given in Section III-A2.

1) Aliasing: When Nyquist-Shannon sampling conditions are violated, all frequency components higher than the Nyquist frequency fall back to the first Nyquist band. This phenomenon is called aliasing. To exemplify the aliasing phenomenon, consider an analog signal, y_{sig}, sampled at a rate f_s with N_s samples. Its discrete (digital) frequency spectrum obtained through a discrete Fourier transform (DFT) is symmetrical around half the sampling rate represented by $N_s/2$. Its frequency resolution, f_{res}, is equal to f_s/N_s, while its repetition frequency is f_s, represented by N_s. The output spectrum of the DFT, z_{sig}, is written as

$$z_{sig}(k) = \sum_{n=0}^{N_s-1} y_{sig}(n) \exp\left(-j\varphi_k n\right), \tag{1}$$

where k goes from 0 to N_s-1, and φ_k is the discrete angle relating the index k of a frequency component of the spectrum, f_k, to the index N_s of the sampling frequency. φ_k is written as,

$$\varphi_k = \frac{2\pi k}{N_s} = \frac{2\pi f_k}{f_s}. \tag{2}$$

As the exponential component in (1) is periodic with a period 2π, equivalent to $k = N_s$, (1) can be adjusted to represent spectral components (analog) outside the Nyquist band.

Based on the adjusted (1) and on (2), the effect of aliasing can be derived. Figure 7 presents the polar representation of frequencies f_k relative to f_s. As shown, all the frequencies that belong to the odd Nyquist bands, $(q-1)\pi \leqslant \varphi_k \leqslant q\pi$ with q = 1, 3, 5, ..., alternatively $(q-1)/2 \leqslant k/N_s \leqslant q/2$, will alias back indistinguishably to the first Nyquist band, $0 \leqslant \varphi_k \leqslant \pi$ or $0 \leqslant k/N_s \leqslant 1/2$, with a translation of $(q-1)\pi$ and the same complex form. On the other hand, all the frequencies that belong to the even Nyquist bands, $(q-1)\pi \leqslant \varphi_k \leqslant q\pi$ with q = 2, 4, 6, ..., alternatively $(q-1)/2 \leqslant k/N_s \leqslant q/2$, will alias back to the first Nyquist band in a mirrored form relative to the Nyquist frequency, with a translation of $(q-2)\pi$ and a conjugate complex form. Such aliasing phenomenon is exemplified in Fig. 8, where frequency bins $N_s/2 - k + pN_s$ and $N_s/2 + k + pN_s$, with $p \in \mathbb{N}$, are transformed to the same digital bin $N_s/2 - k$.

Aliasing phenomenon can have positive or negative effects on measurement systems. As will be shown in the following sections, aliasing can be used to reduce the requirements on

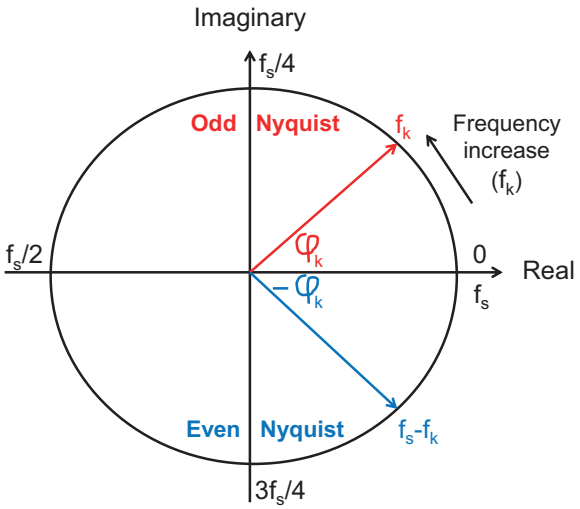

Fig. 7: Polar representation of analog signals in function of the sampling frequency. In red is the polar representation of frequencies in odd Nyquist zones. In blue is the polar representation of frequencies in even Nyquist zones.

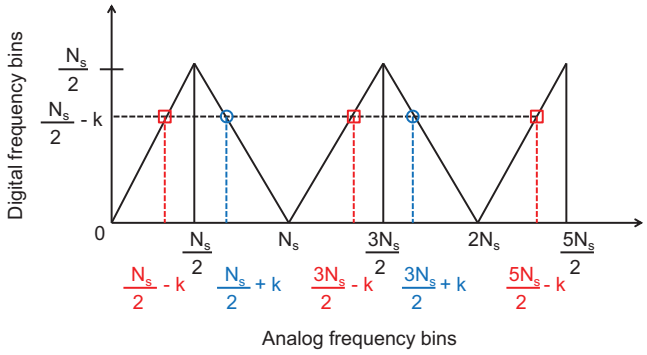

Fig. 8: Aliasing phenomena: representation of digital frequency bin components in function of their analog counterparts. In red are frequencies in odd Nyquist zones and in blue are frequencies in even Nyquist zone.

the sampling rate for some applications, or it can present a difficult challenge for others.

2) Critical tones (origins and effects): As mentioned earlier, a strict version of the Nyquist-Shannon sampling criterion omitted the equality in the lower bound of the sampling rate in order to avoid amplitude and phase ambiguities when measuring waveforms with frequency components at the Nyquist frequency. Unfortunately, such ambiguities also exist at all frequency components that are multiples of the Nyquist frequency [19], [20]. Below is a mathematical explanation of the source of those ambiguities and why frequencies at multiples of the Nyquist frequency are that critical.

Consider a continuous signal of the form

$$s(t) = \sqrt{A^2 + B^2}\sin\left(2\pi f t + \arctan\frac{B}{A}\right), \qquad (3)$$

it can be written as

$$s(t) = A\cos(2\pi f t) + B\sin(2\pi f t). \qquad (4)$$

Consider the case where f is an integer multiple m of $f_s/2$, and the signal is sampled with $t = n/f_s$, where $n = 1, 2, 3, \ldots$. This gives

$$s(n) = A\underbrace{\cos(m\,n\,\pi)}_{(-1)^n \text{ or } 1} + B\underbrace{\sin(m\,n\,\pi)}_{0}, \qquad (5)$$

where the result of the first term depends on whether m is odd, or even. That is, $s(n)$ is an alternating sequence $\pm A$, or a constant A. In particular, the result is independent of B.

In general the sampled signal $s(n)$ is uniquely determined by the pair $(A,\ B)$. However, for the isolated cases where the signal frequency is a multiple of the Nyquist frequency, the sampled signal is independent of B, and an amplitude/phase ambiguity occurs in the reconstruction of the signal from its samples.

Such amplitude/phase ambiguities raise a major challenge for measurement receivers based on undersampling, when the spectrum of the wide-band waveform to measure spreads over multiples of the Nyquist frequency [21]. Hence, those frequencies are denoted as critical frequencies or tones.

B. Undersampling

Since ADCs suffer from a trade-off between sampling rate and resolution, undersampling has been considered as an alternative for measuring wide-band waveforms in some applications, where the sampling rate is smaller than the waveform bandwidth. The aliasing phenomenon, which is considered as an artifact of a badly conditioned measurement, i.e. measuring while violating Nyquist-Shannon condition, can be used in some scenarios to perfectly reconstruct the undersampled waveform. However, as the sampling operation is done at a slow rate, undersampling cannot be used for measuring real-time signals. Instead, it is used for measuring repetitive or periodic signals.

It should be noted that Shannon sampling theorem is referred to sometimes as bandpass sampling or also undersampling. In fact, Shannon sampling theorem is based on the aliasing phenomenon, however, with the condition that the sampling frequency is bigger than twice the bandwidth of the signal to measure. Hence, it can be used in real-time measurements.

In the following, two techniques that had a major impact on some of state-of-the art wide-band RF measurement receivers are reviewed. In addition, a sampling technique, which can be seen as a mixture of undersampling and nonuniform sampling, is presented due to its expected impact on some state-of-the-art wide-band RF receivers.

1) Harmonic sampling: As mentioned previously, undersampling a waveform causes aliasing phenomenon. Hence, all frequency components that are higher than the Nyquist frequency fall back to the first Nyquist zone. This phenomenon is in general destructive due to overlapping of the aliased frequency components. Hence, they can not be separated, and the original waveform cannot be reconstructed correctly from its samples. The harmonic sampling (HS) solves the overlapping problem for sparse waveforms.

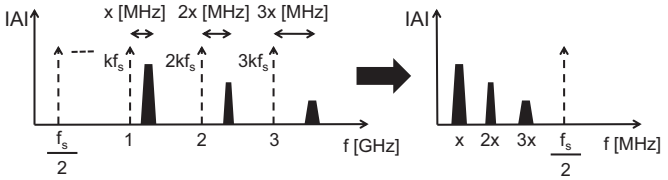

Fig. 9: Example showing the use of HS to measure 3 harmonics. The sampling frequency is chosen such that the 3 harmonics alias back equidistantly to the first Nyquist band.

HS is a process that compresses a wide-band spectrum into a relatively smaller band aliased image. By choosing the relation carefully between the sampling rate and the frequencies of the spectral tones, the reconstruction of the original spectrum can be successful in case of a sparse spectrum whose spectral components are largely distanced and have relatively small bandwidths [22]. Such a sampling strategy is the key-to-success for some of the state-of-the art nonlinear measurement systems, e.g. LSNA [6]. The HS principle is exemplified in Fig. 9 where the aim is to measure a wide-band waveform consisting of three harmonics. The sampling frequency is chosen such that all the harmonic frequencies fall back to the first Nyquist zone equidistantly. The spectrum of the measured data is a compressed version of the original spectrum. Reconstructing the original wide-band spectrum is straight forward through a frequency-based descrambling algorithm and phase correction for the harmonics aliased from even Nyquist zones. Doing an inverse fast Fourier transform (IFFT) operation results in the time domain wide-band waveform.

Such sampling technique, which is referred to as HS down-conversion, is easy to implement when using sparse spectrum with narrow-band individual sub-carriers as in Fig. 9 and when the positions of the spectrum components are known. However, with the recent demands on capturing a dense spectrum whose bandwidth surpass multiples of the Nyquist band, choosing the right sampling frequency tends to be obscure. As a result, overlapping of aliased bins and ambiguities in critical frequencies are highly probable.

2) Equivalent time sampling: As opposite to HS which consists of a frequency-based reconstruction algorithm, equivalent time sampling (ETS) is a sampling technique that uses a time-based reconstruction algorithm to reconstruct an undersampled waveform after accumulating its samples over several repetition periods. The samples can be in order, or scrambled over the time axis. An advantage of ETS over HS is its independency of the spectrum components positions and their sparsity characteristics. Hence, it has a more general use. However, it still requires the knowledge of the waveform repetition rate. ETS is an emerging sampling theory in the world of digital oscilloscopes aiming on measuring a known high-frequency repetitive waveform with a higher effective sampling rate. In addition, ETS can be used as an equivalent oversampling technique for achieving sampling rates in the order of hundreds of GHz.

ETS, as known today, has two strategies for accumulating the samples over time: random accumulation or sequential accumulation. Their main characteristics and method of working

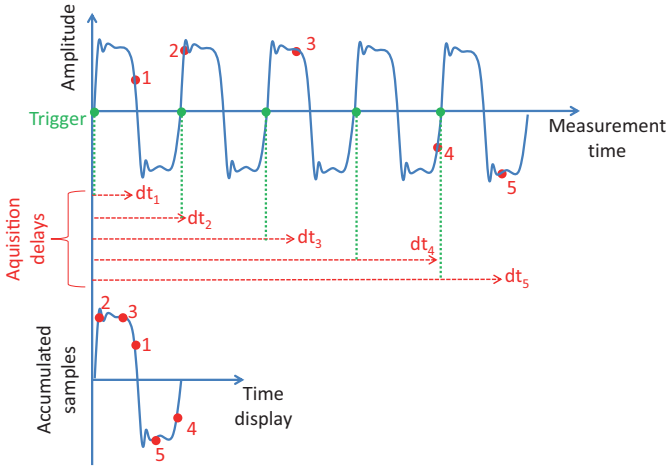

Fig. 10: Example showing the use of random ETS as used in DSOs. The samples are measured randomly with respect to the trigger position. The measured samples are then accumulated on the display based on their known position over the time axis.

are described in the following paragraphs.

a) Random equivalent time sampling:
Random accumulation is well known in the world of digital sampling oscilloscope (DSO) [23]. It is based on taking samples of the input signal in a random way with respect to the sampling trigger. A random ETS uses an internal sampling clock that is incoherent (asynchronous) with the trigger signal. The trigger signal itself is locked to the repetition rate of the measured input signal. Hence, by sampling sequentially in time and independently of the trigger pulses, a randomness is created between the samples and the trigger. However, as both sampler and trigger are controlled, the random delays between them are known. As a result, the samples are accumulated on the display based on their known position over the time axis as presented in Fig. 10.

The main advantage of using random ETS is the ability to measure and display samples before the triggering operation occurs, which gives insights into the sharp edges of the input signals. In a regular triggering scenario, the sampling operation occurs after the trigger pulse is fired. Hence, a sharp edge at the beginning of the signal cannot be measured, which reduces the operating bandwidth of the measurement system. In addition, when measuring slowly repetitive waveforms, random ETS allows capturing several samples per trigger period. Hence, the displayed samples accumulate in a faster way. However, such a sampling strategy has a drawback when measuring fast repetitive waveforms, i.e. triggering at a fast rate, as more than one triggering period is required to collect a sample. As a result, the display process of the measured samples is very slow. In addition to the limitation on measuring fast repetitive waveforms, random ETS is sensitive to jitter and time drift between the trigger and the sampler. Such time distortion affects the accuracy of the random delays, which reduces the resolution of the system [23].

b) Sequential equivalent time sampling:
The second strategy for accumulating the samples over the waveform repetitions is to take one or multiple samples per

period in a well-defined and sequential way. Such a sampling strategy requires the knowledge of the waveform repetition rate, either defined by the user or using a clock recovery module. Sequential ETS is implemented nowadays in two ways which are described in the following paragraphs.

b1- Sequential ETS as used in DSOs:

DSOs implement sequential ETS in such a way that one sample in each repetition of the waveform is measured [23]. This is achieved by inserting an incremental delay between the trigger and the sampler. The trigger itself is set to fire a pulse at the beginning of every repetition of the waveform. For example, the second time the sampler receives a trigger pulse, it waits for a certain delay dt before taking a sample. The third time the sampler receives a trigger pulse, it waits for a delay of $2dt$ before taking a pulse. The process of taking samples continues until all the 'desired' samples of the waveform are measured. The value of the inserted delay dt sets the equivalent sampling period at which the signal will be reconstructed. The samples, which were measured over several periods, are then compressed on the time axis and represent one period of the equivalently sampled/oversampled waveform as shown in Fig. 11. As a consequence, the sampling frequency f_s is lower than the repetition frequency f_r of the waveform, and the achieved equivalent sampling frequency f_{eq} is equal to N_s times f_r, where N_s is the number of samples 'desired' in a measured period of the waveform. Due to such slow sampling technique, N_s periods of the waveform need to be measured with f_s in order to reconstruct one equivalent period as if measured with f_{eq}.

Analytically speaking, consider T_r to be the repetition period of the waveform, T_s the sampling period, and T_{eq} the equivalent sampling period. The sequential ETS process described above can be written as

$$T_s = T_r + T_{eq}. \tag{6}$$

As T_r=$N_s T_{eq}$, (6) can be written as

$$T_s = T_r(1 + \frac{1}{N_s}). \tag{7}$$

Hence, the sequential ETS sampling frequency can be found as

$$f_s = f_r(\frac{N_s}{N_s + 1}). \tag{8}$$

Alternatively,

$$f_{eq} = f_s(N_s + 1). \tag{9}$$

It should be mentioned, that depending on the DSO design requirements, one sample could be measured every multiple of the repetition period. Hence, a sampling clock in the order of kHz can be used, while achieving an equivalent sampling rate in the order of several GHz [24], [25].

From a DSO point of view, the main advantage of using sequential ETS is the simplicity of implementation as compared to random ETS. In fact, generating short and highly precise delays is easier than measuring random delays between a sampler and a trigger as used in random ETS [23]. Still, calibration and accurate triggering is required for high resolution which can be degraded due to jitter, time base distortion and drift

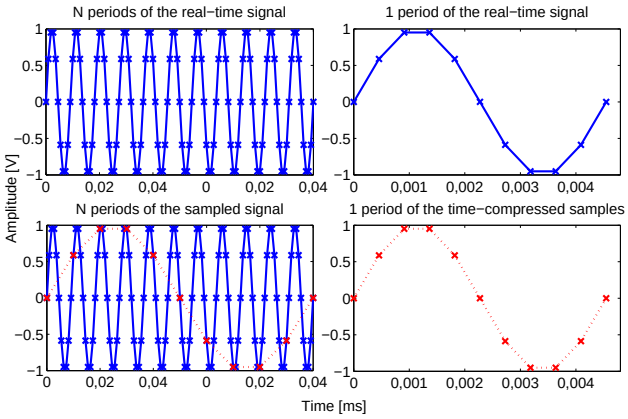

Fig. 11: Example showing the use of sequential ETS as used in DSOs. The equivalent sampling frequency achieved is 12 times the sampling frequency used for digitizing, i.e. N_s=11. In red 'x' are the samples measured with f_s and time-compressed to form one period as if measured with f_{eq}. In blue 'x' are the real-time samples measured with a frequency equal to f_{eq}.

[26]. In addition, sequential ETS can suffer from the critical tones if the waveform contains frequencies that are multiple of half the sampling frequency.

b2- Sequential ETS as used in IEEE Standard 1241:

The second way of implementing sequential ETS can be found in [27] for testing ADCs. It is based on capturing, sequentially and in a well defined manner, more than one sample per repetition period, e.g L samples/repetition. As in the first method, the repetition frequency of the waveform needs to be known, and its relation with the sampling frequency f_s needs to be well defined. The time required for measuring the complete waveform is D times smaller than the time required in the first method, with D=N_s/L and N_s the desired number of samples in a period of the waveform. Because L samples are measured per repetition, f_s is bigger than the repetition frequency of the waveform and the equivalent sampling frequency f_{eq} is D times bigger than f_s. Due to the fact that more than one sample is taken in every repetition, an algorithm to rearrange the samples positions in time in order to reconstruct one oversampled period, is required. An example showing sequential ETS with multiple samples per repetition is presented in Fig. 12.

As in the first method, accurate triggering is essential between the sampling clock and the sampler in order to achieve correct reconstruction. Hence, the performance of the method is affected by jitter, time base distortion and drift. In addition, sequential ETS suffer from the critical tones.

3) Evolved Harmonic sampling: In order to overcome the limitations of HS for measuring a wide-band and dense spectrum whose bandwidth surpasses multiples of the Nyquist frequency, and in order to overcome the limitations of ETS with respect to critical tones, knowledge of the repetition of the waveform, jittering and time-base distortion, a method called evolved harmonic sampling (EHS) has been introduced in [28]. EHS is based on breaking the relation between the undersampling frequency to use and the resolution frequency of the spectrum to measure. Hence, by choosing a sampling

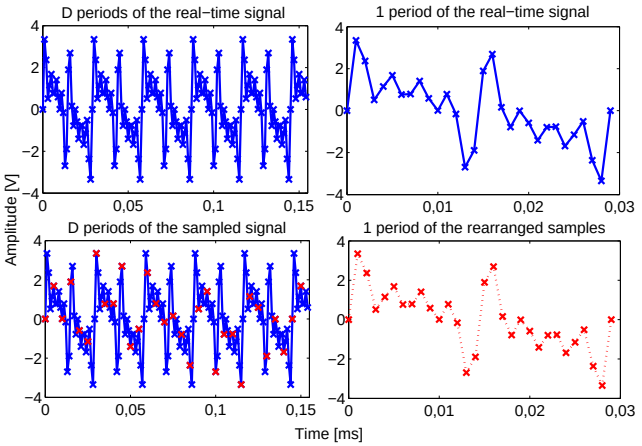

Fig. 12: Example showing the use of sequential ETS while measuring multiple samples per repetition period of the waveform. The equivalent sampling frequency achieved is five times the sampling frequency used for digitizing, i.e. D=5. In red 'x' are the samples measured with f_s and rearranged to form one period equivalently measured with f_{eq}. In blue 'x' are the real-time samples measured with a frequency equal to f_{eq}.

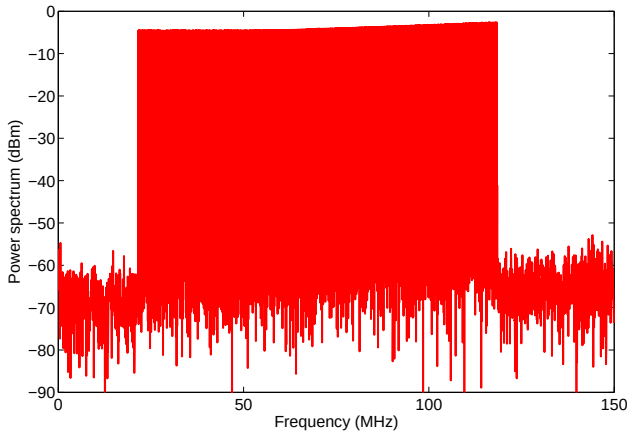

Fig. 13: Example EHS: Reference spectrum of 150 MHz bandwidth measured with 300 MHz sampling frequency and 4096 samples.

frequency with an irrational property, or a quasi-irrational one, it is possible to alias all the frequency components of the spectrum to measure to the first Nyquist band without overlapping. In addition, as no frequency component of the spectrum is a multiple of the Nyquist frequency, the problem of the critical tones is also avoided. Hence, by using a descrambling algorithm [28], the wide-band spectrum is reconstructed accurately. In [28], he authors have presented an algorithm which, for any desired bandwidth and resolution frequency to measure, gives a sampling frequency (within the capabilities of the ADC to use) and a number of samples that can be used to undersample the signal without overlapping in its aliased spectrum. The method of EHS is exemplified in the following by measuring a wide-band waveform using a much smaller sampling frequency than its bandwidth.

A flat multisine signal of bandwidth 100 MHz and centered at 70 MHz is to be measured. The multisine is first measured by a 14-bits ADC with a sampling frequency of 300 MHz and number of samples 4096. The spectrum of the

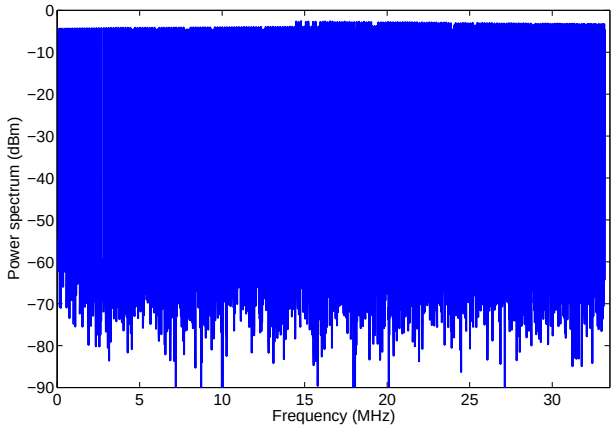

Fig. 14: Example EHS: Undersampled spectrum of 150 MHz bandwidth measured with 66.3867188 MHz and 4532 samples.

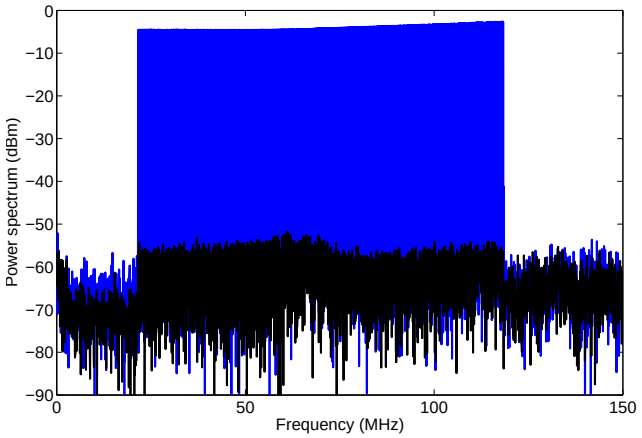

Fig. 15: Example EHS: (blue) Reconstructed spectrum from scrambled undersampled data; (black) Spectrum of the reconstruction error.

oversampled signal will be used as the reference and its power spectrum is shown in Fig. 13. The waveform is then measured with an undersampling frequency of 66.3867188 MHz and a number of samples 4532 obtained from the algorithm in [28]. Its power spectrum is shown in Fig. 14. One should notice that the Nyquist bandwidth 33.1933594 MHz is much smaller than the reference spectrum bandwidth (150 MHz) and the multisine bandwidth (100 MHz). Both reference and undersampled spectrum have a signal-to-noise and distortion ratio in the range of 50 dB after coherent averaging over 100 periods of the data. Descrambling the spectrum of the undersampled data based on the algorithm presented in [28] allows reconstructing the original spectrum which is presented in Fig. 15. In addition, Fig. 15 shows in black color the power spectrum of the reconstruction error; the spectrum of the difference between the reference signal and the reconstructed signal after synchronization to the same time reference plane. It has a normalized mean square error (NMSE) of -49.4 dB, which highlights an accurate reconstruction.

C. Compressive sampling

Due to the rising need of fast samplers for wide-band applications, researchers are investigating new sampling tech-

niques based on advanced signal processing, which violate the Nyquist-Shannon conditions but are still able to give an accurate representation of the digitized signal. In recent years, there has been considerable interest in the information theoretic community regarding the sparsity characteristic of a signal, and its direct application to the field of solving underdetermined systems. In particular, a signal, which can be represented as sparse in a certain domain (e.g., time, frequency, wavelet), can be accurately reconstructed from only few of its samples. This theory is called compressive sampling, or compressive sensing, and is finding its way to the signal processing community with direct application to RF measurement receivers [29]–[31].

Starting from the definition of sparsity, a vector is called sparse if only few of its samples contain information, while the rest are redundant. Such characteristic is well present in wireless signals where the spectrum consists of multiple narrow-band modulated channels spreading over a wide spectrum. Hence, only a small portion of today's spectrum contains information, while the remaining part is either unused or reserved for military and governmental uses. Another relevant application where sparsity can be used, is testing of RF devices using periodic signals, e.g., using multisines. As a result, compressed sampling takes advantage of the sparsity characteristic of an RF spectrum, and uses it to reduce the number of samples required for measuring the whole spectrum. Such reduction in number of samples can be directly related to the reduction in the sampling rate required for measuring a complete wide-band signal. Hence compressive sampling reconstructs accurately the spectrum of a waveform from very few time domain samples by solving an underdetermined system based on ℓ_1-minimization algorithms which reconstruct the sparsest solution with low computational complexity [32]–[36]. A general description of a compressive sampling problem is presented in the following.

Consider the general problem of reconstructing a vector $\mathbf{x} \in \mathbb{R}^N$ from a vector $\mathbf{y} \in \mathbb{R}^M$, such that $M < N$,

$$\mathbf{y} = \Psi\mathbf{x}, \tag{10}$$

where $\Psi \in \mathbb{R}^{M\times N}$ is the sensing, or measurement, matrix. The vector $\mathbf{x}$, which represents a time domain signal, e.g. a multisine, can be written as a function of a sparse vector $\mathbf{z} \in \mathbb{C}^N$ in the frequency domain by means of an IFFT,

$$\mathbf{x} = \Phi\mathbf{z} \tag{11}$$

where $\Phi \in \mathbb{C}^{N\times N}$, called sparsity matrix, is the IFFT matrix operator. Hence (10) can be written as

$$\mathbf{y} = \Psi\mathbf{x} = \Psi\Phi\mathbf{z} = \mathbf{H}\mathbf{z}, \tag{12}$$

where $\mathbf{H} \in \mathbb{C}^{M\times N}$, is generally called the compressive sensing (CS) matrix.

Vector $\mathbf{z}$ is S-sparse, hence having only S coefficients containing information. It has a sparsity level of S/N. As a consequence, $\mathbf{x}$, which represents a multisine in this work, consists of $S/2$ sines. It should be noted that a sparse spectrum has low sparsity level, while a dense spectrum has high sparsity level.

It was shown in [34] that a correct recovery of $\mathbf{z}$ from $\mathbf{y}$ can be achieved with high probability if $\mathbf{H}$ satisfies the restricted isometry property (RIP) [34], and

$$M \geqslant CS\log(\frac{N}{S}), \tag{13}$$

where C is a user defined constant that sets the optimum performance of the bound in (13). The probability of correct recovery tends to one when M is much larger than its lower bound presented in (13) or when the spectrum is highly sparse. Several forms exist in the literature regarding the lower bound on the number of measurement points M, (13), which give, with high probability, a correct solution for the underdetermined problem presented in (12). Those lower bounds and their constants 'C', depend highly on the characteristics of the matrix $\mathbf{H}$, and on the reconstruction algorithms that are used. It was shown in [37] and [38] that random matrices satisfy RIP. Hence, if Ψ has random properties, the exact solution of (12) can be found by solving an ℓ_1-minimization problem [35],

$$\min\|\widehat{\mathbf{z}}\|_1 \qquad \text{subject to} \qquad \mathbf{H}\widehat{\mathbf{z}} = \mathbf{y}, \tag{14}$$

with $\|\cdot\|_1$ being the ℓ_1-norm. The problem in (14) is convex and can be solved by several existing algorithms [39]. However, for large dimension problems, iterative greedy search algorithms can be faster, e.g. [32], [33] and [36].

Compressive sampling performs perfectly if the measurement operation randomizes the signal to measure prior to sampling or randomize the way it samples the signal. Several research groups have suggested measurement setups to implement compressive sampling for the purpose of reducing the sampling rate in receivers. The majority of the implemented compressive sampling prototypes were based on the random demodulator (RD) [40] or the modulated wide-band converter (MWC) [41], and require the use of a large number of parallel sampling front-ends which raise questions regarding their applicability. In addition, those implemented prototypes require the design and accurate characterization of analog devices such as wide-band sliding time window integrators[1], wide-band mixers and equalizers. Hence, in their current development stage, they suffer from hardware complexity. An example of such measurement setups is given in Fig. 16.

Lately, a cost efficient measurement setup designed for measuring wide-band periodic sparse waveform has been introduced [43]. It allows measuring a wide-band periodic sparse signal of bandwidth JK GHz, $J \in \mathbb{N}$, using only one ADC with an analog bandwidth of K GHz and a sampling rate of a few MHz. Its simplified block diagram is presented in Fig. 17.

The measurement strategy presented in [43] is based on splitting the waveform to be measured into parallel frequency-band channels, then downconverting them to the analog frequency band of the ADC, i.e., which is up to here similar to the digital bandwidth interleaving technique [8]. The parallel signals are then randomized by multiplying them with pseudo-random (PN) sequences, summed, and measured using one

[1]A sliding time window integrator slows down the rate of a signal, hence compresses its bandwidth [42].

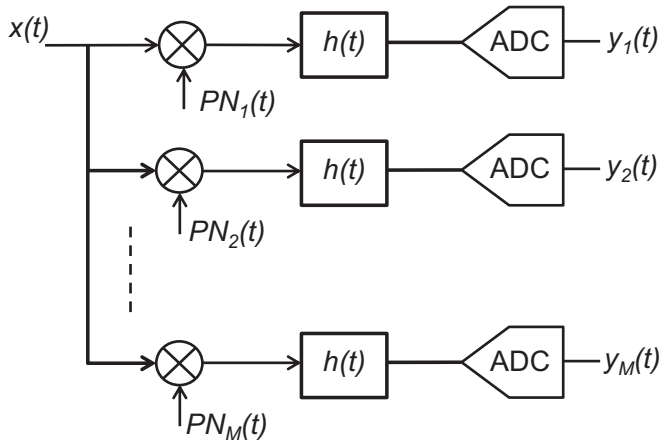

Fig. 16: An example of measurement setups implementing compressive sampling. Several copies of the signal are first randomized through mixing with a pseudo-random (PN) sequence, then filtered or integrated, and finally measured by an ADC at a sampling rate smaller than the bandwidth of the original signal [40], [41].

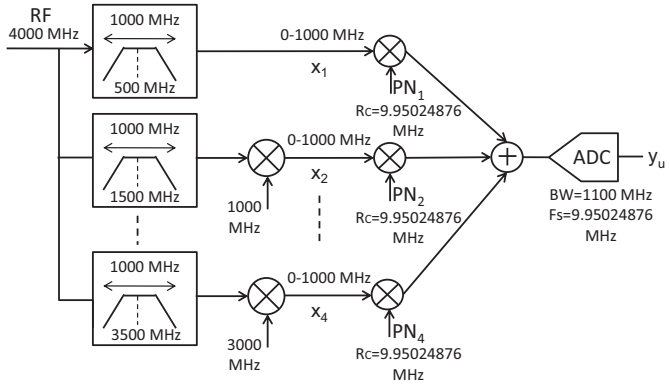

Fig. 17: Simplified measurement setup used for capturing a 4000 MHz periodic sparse waveform with a 1100 MHz analog bandwidth ADC running at 9.95024876 MHz.

ADC. The reason behind multiplying the signals with PN-sequences is to design a measurement matrix with random properties. For measuring periodic waveforms, EHS is used on both PN-sequence and ADC levels in order to reduce respectively their chipping and sampling rate down to few MHz. Major advantages of using EHS at the PN-sequence level are to overcome jitter and triggering problem, and to avoid spectrum spreading of the signals due to multiplication by the PN-sequences which puts tough requirements on the analog and digital bandwidth of the ADC to use.

In order to separate and reconstruct the parallel signals from the measured data, the sparsity characteristic of the signals is used. Hence, a reconstruction algorithm is designed in [43], which searches for the sparsest solution. The reconstructed parallel signals are then joined together to form the original wide-band waveform. The performance of the measurement setup for 2 and 4 parallel channels are validated in [43] over 1000 Monte-Carlo repetitions for a reconstruction error below -80 dB. The results reported in [43] show 100% probability of success when the sparsity levels are below 35.3% and 13.9% for 2 and 4 channels respectively.

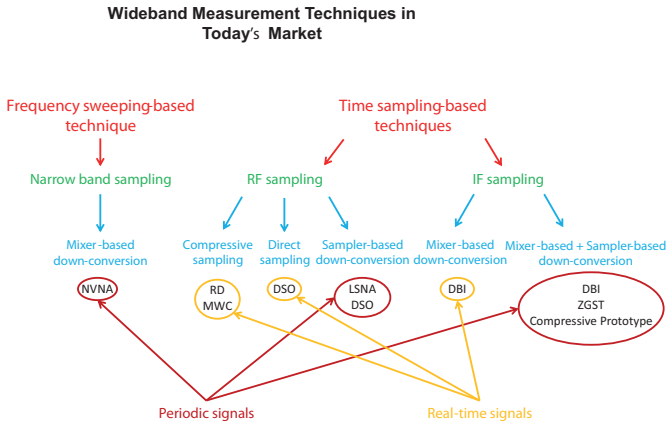

Fig. 18: Major wide-band measurement techniques existing in today's market.

IV. Conclusion

Since Nyquist-Shannon sampling criteria was introduced, a lot of theories have been developed and many measurement systems have been designed to achieve the most accurate measurement of a broadband telecommunication signal. Over the years, the measurement bandwidth of the instruments has increased exponentially from the kHz scale to the GHz scale. The dynamic range has improved from less than 10 dB to more than 100 dB. Many techniques to overcome the analog hardware limitations have been successfully introduced and theories to reduce the required amount of measured data and hardware complexity are being investigated. From measuring periodic signals to real-time signals, based on narrow-band sampling to RF-sampling, using frequency sweeping-based techniques to time sampling-based techniques, several measurement instrumentation have been introduced in the market Fig. 18. As can be noticed, sampling-based instrumentation are dominating today's market with enhanced bandwidth and dynamic range, faster processing time, and wider range of applications. Despite the large dynamic range that current sweeping-based instruments offer, it is anticipated that with the ongoing improvements on the dynamic range, RF sampling-based instruments with wide-band real-time measurement capabilities, such as enhanced sampling oscilloscopes with multiple synchronized ports, will take the lead in nonlinear measurements.

Will the sampling theory evolve more in the future? For sure, more bandwidth will be achievable with higher resolution and larger memory capabilities to store and collect data, due to the continued improvements in the IC/DSP technology development and the never ending greedy demands for more performance. But, will this be needed? Only the future trends of wireless communication systems will bring council.

References

[1] Rohde & Schwarz. [Online]. Available: http://www.rohdeschwarz.com/.
[2] Agilent Technologies. [Online]. Available: http://www.agilent.com/.
[3] Anritsu. [Online]. Available: http://www.anritsu.com/.
[4] W. Van Moer and L. Gomme, "NVNA versus LSNA: enemies or friends?" *IEEE Microwave Magazine*, vol. 11, no. 1, pp. 97–103, February 2010.

[5] J. Verspecht, "The return of the sampling frequency convertor," in *ARFTG Microwave Measurements Conference, 2003. Fall 2003. 62nd*, December 2003, pp. 155–164.

[6] J. Verspecht, "Large-signal network analysis," *IEEE Microwave Magazine*, vol. 6, no. 4, pp. 82–92, 2005.

[7] D. Williams, P. Hale, and K. Remley, "The Sampling Oscilloscope as a Microwave Instrument," *IEEE Microwave Magazine*, vol. 8, no. 4, pp. 59–68, August 2007.

[8] P. Pupalaikis, "Digital Bandwidth Interleaving," *White paper, LeCroy*, April 2010.

[9] R. Shimon, B. Asay, D. Dascher, K. Griggs, C. Rehorn, M. Adamski, E. Ehlers, C. Hutchinson, and B. Doerr, "InP IC Technology Powers Agilent's Infiniium 90000 X-Series Real Time Oscilloscope," in *IEEE Compound Semiconductor Integrated Circuit Symposium*, October 2010, pp. 1–4.

[10] O. Andersen, N. Björsell, and N. Keskitalo, "A test-bed designed to utilize zhu's general sampling theorem to characterize power amplifiers," in *IEEE Instrumentation and Measurement Technology Conference*, May 2009, pp. 201–204.

[11] LeCroy. [Online]. Available: http://www.lecroy.com/.

[12] W. Kester, *Analog-Digital Conversion*. Analog Devices, 2004.

[13] W. Kester, "Sample-and-Hold Amplifiers," *Tutorial, MT-090, Analog Devices*, 2009.

[14] N. Gray, *ABCs of ADCs: Analog-to-Digital Converter Basics*. National Semiconductor, 2006.

[15] B. Widrow and I. Kollár, *Quantization Noise: Roundoff Error in Digital Computation, Signal Processing, Control, and Communications*. Prentice Hall, 2008.

[16] B. Murmann, "ADC Performance Survey 1997-2011," http://www.stanford.edu/∼murmann/adcsurvey.html.

[17] H. Nyquist, "Certain topics in telegraph transmission theory," *IEE Transactions*, vol. 47, no. 2, pp. 617–644, January 1928.

[18] C. Shannon, "Communication in the presence of noise," in *Proceedings Institute of Radio Engineers*, vol. 37, no. 1, January 1949, pp. 10–21.

[19] V. Ingle and J. Proakis, *Digital Signal Processing Using Matlab*. Brooks/Cole, California, 2000.

[20] R. Lyons, *Understanding Digital Signal Processing*. Prentice Hall, 2004.

[21] C. Nader, B. Björsell, and P. Händel, "Unfolding the frequency spectrum of undersampled wideband data," *Signal Processing*, vol. 91, no. 5, pp. 1347–1350, May 2011.

[22] M. Kahrs, "50 years of RF and microwave sampling," *IEEE Transactions on Microwave Theory and Techniques*, vol. 51, no. 6, pp. 1787–1805, June 2003.

[23] *Sampling oscilloscope techniques*. Tektronix, Technique primer 47W-7209, 1989.

[24] J. Verspecht, "Calibration of measurement system for high frequency nonlinear devices," Ph.D. dissertation, Vrije Universiteit Brussel, 1995.

[25] D. Drickson and M. Muller, *Digital Communications Test and Measurement*. Cambridge University Press, 2008.

[26] T. Clement, P. Hale, D. Williams, C. Wang, A. Dienstfrey, and D. Keenan, "Calibration of Sampling Oscilloscopes With High-Speed Photodiodes," *IEEE Transactions on Microwave Theory and Techniques*, vol. 54, no. 8, pp. 3173–3181, August 2006.

[27] *IEEE standard for terminology and test methods for analog-to-digital converters, IEEE Standard 1241-2010*, IEEE Instrumentation and Measurement Society Std., 2010.

[28] C. Nader, W. Van Moer, K. Barbé, N. Björsell, and P. Händel, "Harmonic sampling and reconstruction of wide-band undersampled waveforms: breaking the code," *IEEE Transactions on Microwve Theory and Techniques*, vol. 59, no. 11, pp. 2961–2969, November 2011.

[29] E. Candès, J. Romberg, and T. Tao, "Robust uncertainty principles: Exact signal reconstruction from highly incomplete frequency information," *IEEE Transactions on Information Theory*, vol. 52, no. 2, pp. 489–509, February 2006.

[30] D. Donoho, "Compressed sensing," *IEEE Transactions on Information Theory*, vol. 52, no. 4, pp. 1289–1306, April 2006.

[31] E. Candès and M. Wakin, "An introduction to compressive sampling," *IEEE Signal Processing Magazine*, vol. 25, no. 2, pp. 21–30, March 2008.

[32] R. Tibshirani, "Regression shrinkage and selection via the lasso," *Journal of the Royal Statistical Society Series B*, vol. 58, no. 1, pp. 267–288, 1996.

[33] S. Sardy, A. Bruce, and P. Tseng, "Block coordinate relaxation methods for nonparametric wavelet denoising," *Journal of Computational and Graphical Statistics*, vol. 9, no. 2, pp. 361–379, June 2000.

[34] E. Candès and T. Tao, "Decoding by linear programming," *IEEE Transactions on Information Theory*, vol. 51, no. 12, pp. 4203–4215, December 2005.

[35] J. Romberg, "Sparse Signal Recovery via l-1 Minimization," in *40th Annual Conference on Information Sciences and Systems*, March 2006, pp. 213–215.

[36] J. Tropp and A. Gilbert, "Signal recovery from partial information via orthogonal matching pursuit," *IEEE Transactions on Information Theory*, vol. 53, no. 12, pp. 4655–4666, December 2007.

[37] R. Baraniuk, M. Davenport, R. DeVore, and M. Wakin, "A simple proof of the restricted isometry property for random matrices," *Constructive Approximation*, vol. 28, no. 3, pp. 253–263, December 2008.

[38] R. Baraniuk and M. Wakin, "Random projections of smooth manifolds," *Foundations of Computational Mathematics*, vol. 9, no. 1, pp. 51–77, February 2009.

[39] S. Boyd and L. Vandenberghe, *Convex Optimization*. Cambridge University Press, 2004.

[40] J. Tropp, J. Laska, M. Duarte, J. Romberg, and R. Baraniuk, "Beyond nyquist: Efficient sampling of sparse, bandlimited signals," *IEEE Transactions on Information Theory*, vol. 56, no. 1, pp. 520–544, January 2010.

[41] M. Mishali and Y. Eldar, "From theory to practice: Sub-Nyquist sampling of sparse wideband analog signals," *IEEE Journal of Selected Topics on Signal Processing*, vol. 4, no. 2, pp. 375–391, April 2010.

[42] X. Chen, Z. Yu, S. Hoyos, B. Sadler, and J. Silva-Martinez, "A Sub-Nyquist Rate Sampling Receiver Exploiting Compressive Sensing," *IEEE Transactions on Circuits and Systems I*, vol. 58, no. 3, pp. 507–520, March 2011.

[43] C. Nader, W. Van Moer, N. Björsell, K. Barbé, and P. Händel, "Reducing the analog and digital bandwidth requirements of RF receivers for measuring periodic sparse waveforms," *IEEE Transactions on Instrumentation and Measurements*, vol. 61, no. 11, pp. 2960–2971, November 2012.